Note

Porosity tuning of carborane-based metal–organic frameworks (MOFs) via coordination chemistry and ligand design

Alexander M. Spokoyny [1], Omar K. Farha [1], Karen L. Mulfort [2], Joseph T. Hupp *, Chad A. Mirkin **

Department of Chemistry and the International Institute for Nanotechnology, Northwestern University, 2145 Sheridan Road, Evanston, IL 60208, United States

ARTICLE INFO

ABSTRACT

Two new metal–organic framework (MOF) materials based on boron-rich cluster struts (*p*-carborane) are reported herein. Cu(I) catalyzed coupling chemistry was used to synthesize carboxylate-based ligands, which are substantially longer than the previously studied dicarboxylated *p*-carborane, leading to structures with greater porosity. Solvothermal syntheses involving these ligands and Zn salts were used to prepare two new Zn(II)-based MOFs with 2D and 3D open framework structures. Upon thermal activation, these MOFs retain the chemical identity of their frameworks, leading to highly porous materials.

© 2010 Elsevier B.V. All rights reserved.

1. Introduction

Coordination chemistry provides a versatile pathway to construct a wide variety of supramolecular assemblies [1]. Metal–organic framework (MOF) materials (i.e. porous coordination polymers) are an emerging class of such structures that are promising for many applications, including small molecule storage, separations, and catalysis [2–4]. Over the past 10 years, there has been significant progress made towards building a library of MOF structures with favorable materials characteristics, including tailorable pore sizes and volumes, low molecular weights, and unsaturated metal coordination sites [5–7]. Control over these parameters is considered to be critical for realizing materials exhibiting high gravimetric uptake of small gas molecules, as well as selective gas separation capabilities [8,9]. However, achieving such control is extremely difficult. Specifically, thermal activation, which is required to generate unsaturated metal sites, often results in irreversible collapse of the porous structure [10,1]. Recently, we developed a series of robust microporous materials based upon icosahedral carboranes [11]. MOFs made from these materials have advantages compared to many aryl-based systems with regard to structural rigidity and thermal and chemical stability [12]. Prior studies have utilized dicarboxylated *p*-carboranyl ligands and

Zn(II) and Co(II) salts to create MOFs and, more generally, infinite coordination polymer (ICP) materials [12,13]. In general, these materials exhibit unprecedented stability with respect to thermal degradation, allowing them to undergo activation by heating under vacuum. Such activation can lead to uncoordinated metal sites in the pores, which significantly enhance hydrogen gas uptake and influence selectivity in gas mixture separation experiments [14–16]. Herein, we report the synthesis of two ligands based on *p*-carborane and the MOF structures prepared from them. These MOFs exhibit significantly higher surface areas than their single carborane predecessors.

2. Results and discussion

We have selectively functionalized *p*-carborane **1** (Scheme 1) to form the rigid, linear precursors **2** and **4** via Cu(I) coupling chemistry, as reported by Michl et al. and Hawthorne et al. [17–19]. The chemical orthogonality of the BH and CH moieties in the carborane unit permits one to selectively derivatize it, which cannot be easily accomplished with polyaryl analogs. Specifically, the acidity of the carborane CH moieties allows them to be lithiated (1.6 M MeLi solution in diethyl ether) and further carboxylated through the addition of excess solid dry CO_2 to the reaction mixture, as was demonstrated previously for *p*-carborane [12]. This carboxylation procedure allows one to prepare ligands **3** and **5** in 78% and 80% yields, respectively. Both **3** and **5** were characterized in solution by ^1H, $C\{^1H\}$, and $^{11}B\{^1H\}$ NMR spectroscopy, and all data are consistent with the proposed structural formulations.

Solvothermal reactions of **3** and **5** with Zn(II) nitrate salt in appropriate solvent mixtures yield crystalline MOFs **6** and **7**, respectively. Both materials were characterized in the solid-state
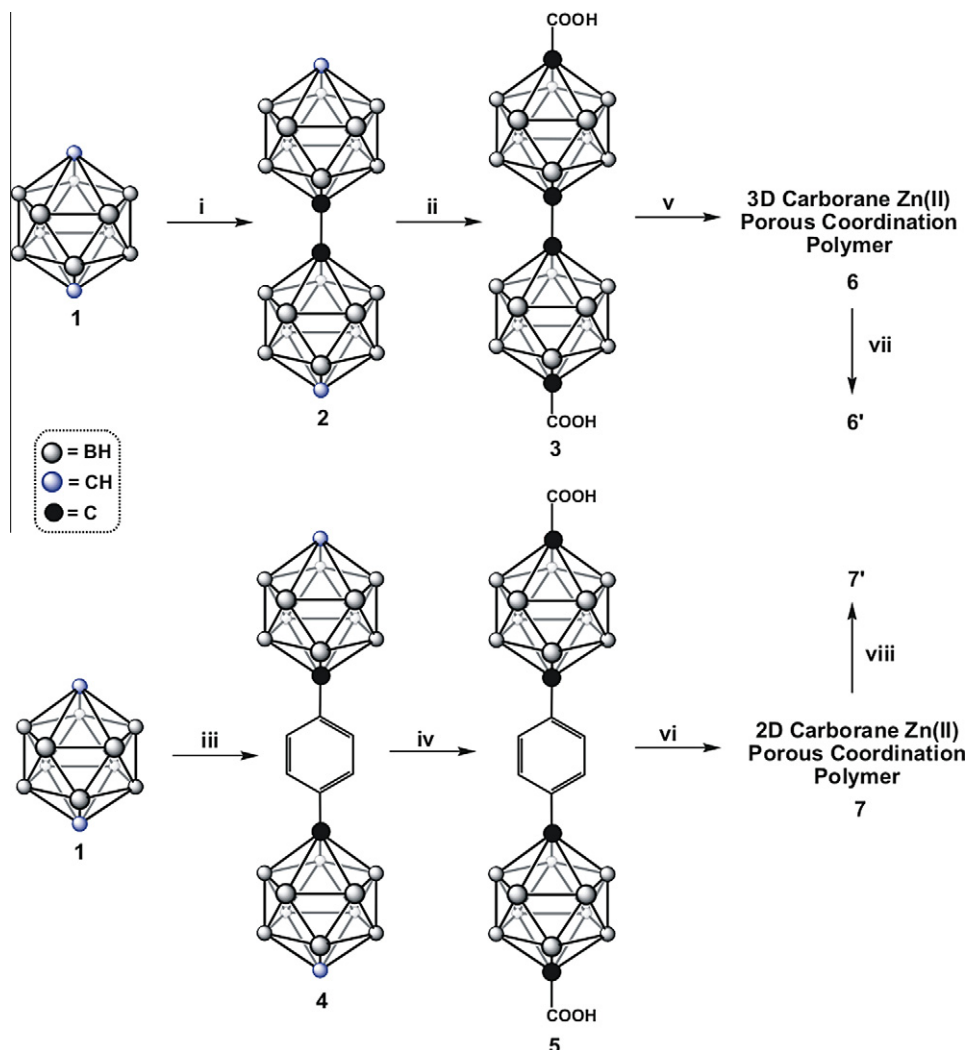
Scheme 1. Syntheses of carborane-based MOFs: (i) ^{n}BuLi, CuCl$_2$, 45%, (ii) MeLi, CO$_2$, ether, 78%, (iii) ^{n}BuLi, CuCl, 1,4-diiodobenzene in THF, then Pd(PPh$_3$)$_2$Cl$_2$ in NMP, 55%, (iv) 1.6 M MeLi, CO$_2$, ether, 80%, (v) Zn(NO$_3$)$_2$·6H$_2$O, DMF/DEF/EtOH, 80 °C, (vi) Zn(NO$_3$)$_2$·6H$_2$O, DMF/DEF/EtOH/H$_2$O, 80 °C, (vii) heat, vacuum, (viii) heat, vacuum.

by single-crystal X-ray diffraction analyses (*vide infra*). MOF **6** was prepared by a solvothermal reaction between Zn(II) nitrate hexahydrate and ligand **3** in a 1:1:1 mixture of dimethylformamide (DMF), diethylformamide (DEF), and ethanol (EtOH). A single-crystal X-ray diffraction study of **6** revealed that it crystallizes in the monoclinic space group, $P2_1/c$. It is a 3D open framework with repeating secondary building units (SBU) comprised of Zn$_4$(OH)$_2$(DMF)$_4$ metal clusters (Fig. 1); ligand **3** serves as a connector between the Zn-based nodes, which binds in two distinct modes, η^1 and η^2 (Fig. 1A).

The asymmetric unit of **6** consists of four Zn(II) ions, three carborane-based ligands **3**, two hydroxy groups, and four DMF moieties (in addition to the disordered solvent molecules trapped in the pores). Within the Zn$_4$(OH)$_2$(DMF)$_4$ clusters (Fig. 1A), two of the four independent Zn(II) ions are hexacoordinated with slightly distorted octahedral environments. Within the SBU, two oxygen atoms come from the η^1- and η^2-bound ligands **3**, two from two hydroxy groups, and two from two DMF molecules. The remaining two crystallographically independent metal centers are tetracoordinated in a slightly distorted tetrahedral environment of the ZnO$_4$ type [5]. One of the three ligands **3**, bridges four Zn(II) ions and connects two adjacent Zn$_4$(OH)$_2$(DMF)$_4$ clusters. The remaining two independent **3** moieties bridge three metal centers from the two adjacent Zn$_4$(OH)$_2$(DMF)$_4$ nodes (in both cases, the non-

coordinated oxygen atom is ∼2.8 Å from the tetrahedral Zn(II) ion already coordinated by the ligand). The hydroxy groups bridge three metal centers within the same cluster, and DMF molecules complete the coordination sphere of the octahedral metal centers.

MOF **7** was prepared by a solvothermal reaction between ligand **5** and Zn(II) nitrate hexahydrate in a 1:1:1:1 mixture of DMF, DEF, EtOH, and water. Single-crystal X-ray analysis revealed that **7**, unlike **6**, is a 2D framework composed of 1D layers stacked in an ABAB arrangement, with a triclinic $P\bar{1}$ space group (Fig. 2). The framework for **7** consists of dinuclear Zn$_2$(H$_2$O)(EtOH) SBU clusters interconnected in a paddle wheel fashion, with four dianionic ligands **5** (η^2 fashion) to form a 2D infinite layer (Fig. 2A). The axial sites of the Zn$_2$-based paddle wheels are occupied by one EtOH molecule on one Zn(II) site (Zn–O distance: 1.977 Å) and one H$_2$O molecule on the other Zn(II) (Zn–O distance: 1.956 Å) in an alternating fashion. Consequently, both of the Zn(II) centers are pentacoordinated in distorted square pyramidal geometries within the Zn$_2$-based cluster. Importantly, solvents coordinated on the Zn(II) sites appear to act as pillars, which stabilize the structure via hydrogen bonding and van der Waals interactions (Fig. 2D).

The phase purity of **6** and **7** prepared in bulk was confirmed by comparing the powder diffraction pattern (PXRD) (Fig. 3). Both of these materials exhibit a strong diffraction pattern, which is characteristic of their high crystallinity. Importantly, the diffraction
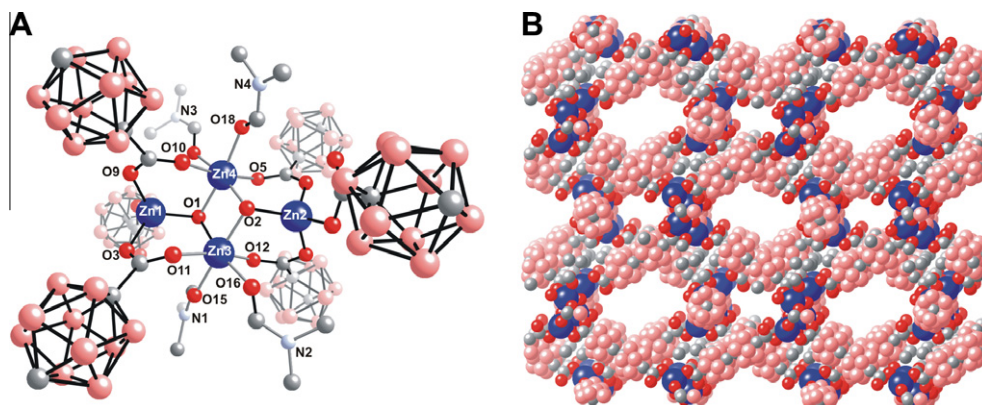
Fig. 1. The crystallographically derived structure of **6**: (A) cluster geometry with ligands (parts of carborane ligands and hydrogen atoms are removed for clarity) and (B) space-filling model of the extended framework without coordinated DMF solvent molecules and hydrogen atoms. In all cases, zinc atoms are dark blue, oxygen atoms – red, boron atoms – salmon, carbon atoms – grey, nitrogen atoms – light blue, and hydrogen atoms – white. (For interpretation of the references in colour in this figure legend, the reader is referred to the web version of this article.)
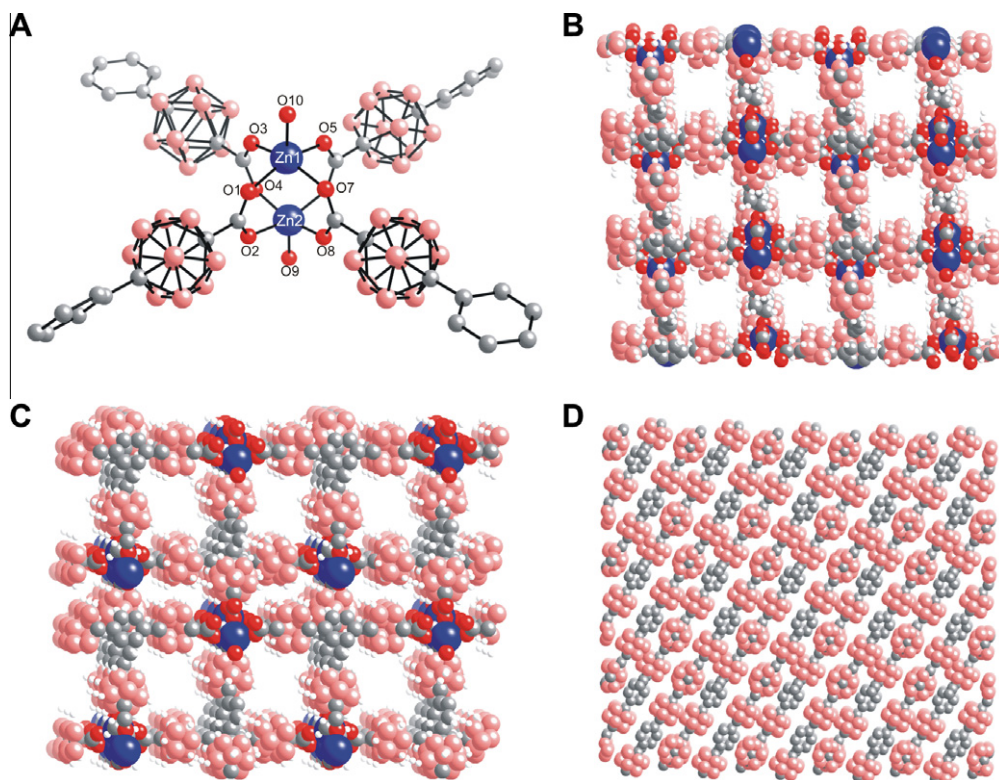

Fig. 2. The crystallographically derived structure of **7**: (A) cluster geometry (parts of carborane ligands and hydrogen atoms are removed for clarity), (B and C) space-filling models of the extended frameworks, and (D) representation of layers. In all cases, zinc atoms are dark blue, oxygen atoms – red, boron atoms – salmon, carbon atoms – grey, nitrogen atoms – light blue, hydrogen atoms – white in color. (For interpretation of the references in colour in this figure legend, the reader is referred to the web version of this article.)

pattern generated from the bulk samples of **6** and **7** match the pattern of the samples generated from single-crystal diffraction data. As suggested by TGA analysis, both **6** and **7** can be activated in a manner that retains their crystallinity. PXRD patterns of the activated materials **6′** and **7′**, respectively, fully supports this observation (see supporting information). Within **6**, clathrated solvent molecules exit the framework between 100 and 170 °C, followed by coordinated DMF molecules in the 240–290 °C temperature range (Fig. 4).

Decomposition of **6** is observed only at 510 °C, which is significantly higher than most Zn(II) aryl-based MOFs (350–400 °C) [20]. A sample of **6** was thermally activated at 250 °C for 20 h under dy-

namic vacuum (0.01 m Torr), providing activated material **6′**. This procedure results in complete solvent loss (both clathrated and coordinated at SBUs), as evidenced by CP-MAS ^{13}C NMR spectroscopy. Indeed, resonances at δ 25 corresponding to DMF molecules are not observed in **6′**, in contrast with the parent material **6**. Resonances corresponding to ^{13}C-atoms in ligand **5** (δ 165 and 75) in **6** and **6′** do not change during activation, suggesting that the framework remains chemically intact. Volumetric gas-sorption measurements of **6′** using N_2 were used to verify its microporosity. Indeed, it exhibits a reversible Type 1 isotherm (Fig. 5A). Importantly, the calculated surface area (Brunauer, Emmett, Teller – BET = 1180 m^2/g) is the largest for any studied carborane-based MOF thus
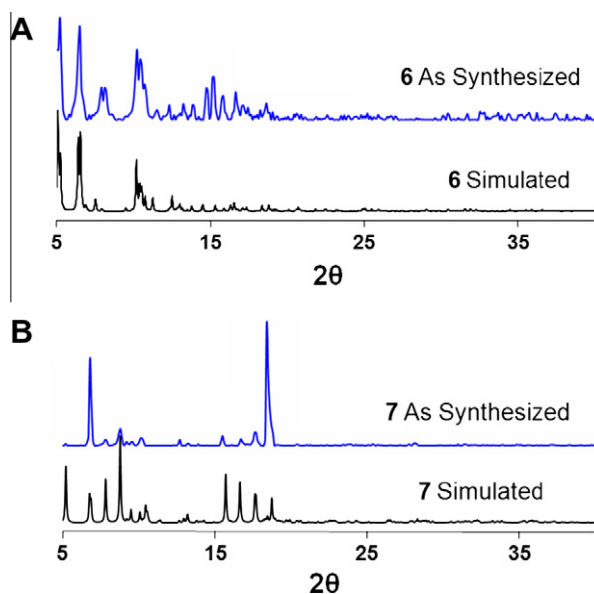
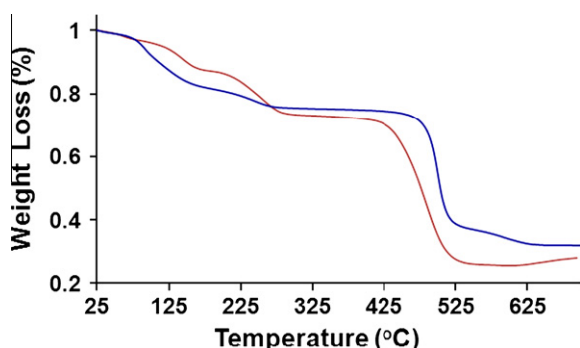**Fig. 3.** Powder X-ray diffraction data for (A) **6** and (B) **7**.

Fig. 4. TGA traces of **6** (blue) and **7** (red). (For interpretation of the references in colour in this figure legend, the reader is referred to the web version of this article.)

far, which is a direct consequence of the extended ligand design approach explored in this work. While it is yet unclear whether upon activation these structures result in a substantial number of open coordination sites being exposed, we are currently working towards probing this possibility spectroscopically via carbon monoxide (CO) binding studies.

Similar to **6**, the TGA data indicate that **7** undergoes solvent-loss mass changes over the 100–160 °C (clathrated molecules) and 180–270 °C (coordinated solvent molecules-water/ethanol) temperature ranges (Fig. 4). The resulting porous framework begins to decompose only above 425 °C. PXRD studies reveal that **7** retains its crystallinity even after solvent molecules have been removed completely. Thermal treatment of **7** under vacuum (200 °C, 15 h, 0.01 m Torr) leads to **7′**, which has a microporosity of 800 m²/g as determined by CO_2 volumetric gas sorption and NLDFT (non-local density functional theory) modeling (Fig. 5B). The stability of material **7** is likely due to its unique stacking structure, which prevents the loss of porosity even when solvent molecules are removed and the layers shift closer to each other.

3. Experimental

3.1. Materials and methods

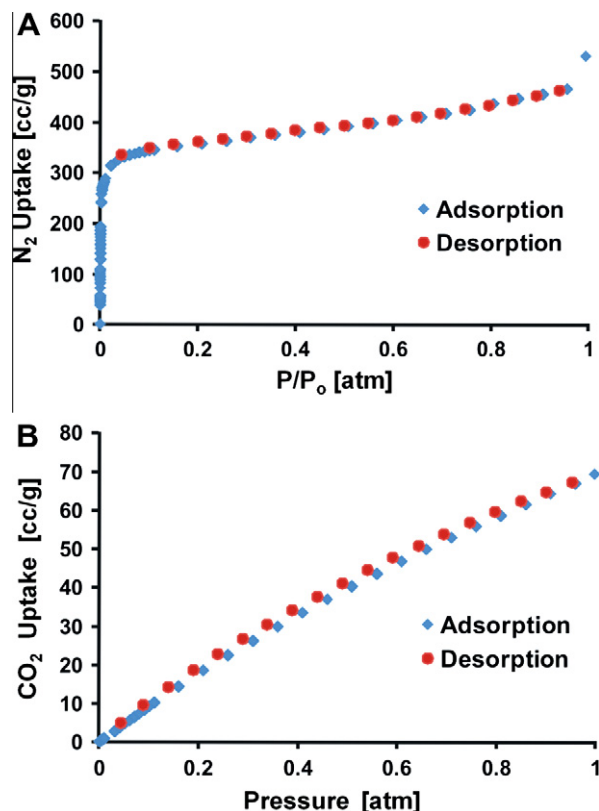Solvents and all other chemicals were obtained from Aldrich Chemical Co. (Milwaukee, USA) and used as received unless

Fig. 5. Volumetric gas-sorption properties of (a) **6′** and (b) **7′**.

otherwise noted. 1,12-Dicarba-closo-dodecaborane (p-carborane) was purchased from Katchem (Czech Republic) and used as received. Compounds **2** and **3** were prepared according to previously published procedures [17–19]. Compound **4** was prepared according to the same procedure reported by Michl et al., where instead of 1,3-diiodobenzene, 1,4-diiodobenzene was used (NMR data for **4**: ^1H NMR (CDCl₃, 400 MHz): δ 6.9 (s, 4H, C**H**), δ 3.4–1.4 (bm, 20H, B**H**), δ 2.75 (s, 2H, cage-C**H**); ^{13}C NMR (CDCl₃, 100 MHz): δ 137.1 (s, aromatic-**C**), δ 126.9 (s, aromatic-**C**H), δ 60.2 (s, B**C**H), $^{11}B\{^1H\}$ NMR (CDCl₃, 128.5 MHz, BF₃-ether): δ −12.5 (s), −14.7 (s)) [18]. Solution NMR data was acquired on Varian Inova 400 instrument equipped with a broadband probe. CP-MAS ^{13}C NMR spectroscopy was done on a Varian Inova 400 Widebore instrument. CHN Elemental Analyses data were obtained from Quantitative Technologies Inc. (Intertek), Whitehouse, NJ. Powder X-ray diffraction (PXRD) patterns were recorded with a Rigaku XDS 2000 diffractometer using nickel-filtered Cu Kα radiation (λ = 1.5418 Å). Thermogravimetric analyses (TGA) were performed on a Mettler-Toledo TGA/SDTA851e. Adsorption isotherms were measured with an Autosorb 1-MP from Quantachrome Instruments.

3.2. Synthetic procedures

Compound **5**. To 610 mg (1.8 mmol) of **4** dissolved in 16 mL of dry diethyl ether and stirred at 0 °C, 1.6 M (4 mL, 6.4 mmol) n-MeLi was added via syringe under nitrogen. The reaction mixture was slowly brought up to room temperature and then refluxed for 1.5 h. The reaction was subsequently cooled to −78 °C on a dry-ice/acetone bath. Carbon dioxide gas was bubbled into the reaction mixture for an hour while stirring. The reaction mixture was then quenched with 25 mL of 6 M hydrochloric acid and extracted with diethyl ether (2×, 50 mL). The combined organic layers were con-

centrated *in vacuo* to yield a crude solid product, which was then washed with excess water and hexanes on a fritted glass filter to yield an off-white solid **5** (600 mg, 78%). ^{1}H NMR (d^8-THF, 400 MHz): δ 7.6 (bs, 2H, COO**H**), δ 7.0 (s, 4H, C**H**), δ 3.4–1.4 (bm, 20H, B**H**); ^{13}C NMR (d^8-THF, 100 MHz): δ 162.7 (s, **C**OOH), δ 136.8 (s, aromatic-**C**), δ 127.0 (s, aromatic-**C**H), δ 83.8 (s, B**C**), δ 78.0 (s, B**C**); ^{13}C NMR (d^8-THF, 100 MHz, DEPT), δ 127.0 (s, aromatic-**C**H).

Compound **6**. Zinc (II) nitrate hexahydrate (Zn(NO$_3$)$_2$·6H$_2$O) (30 mg) and **3** (10 mg) were dissolved in DEF/DMF/ethanol (1:1:1 by volume) in a glass vial and allowed to react at 80 °C for 24 h. Crystals of **6** were collected and washed with DMF and dried at 70 °C under vacuum to afford a white material (60% yield). Elemental analysis: *Anal*. Calc. for (C$_{18}$H$_{62}$B$_{60}$Zn$_4$O$_{14}$)·(4DMF): C, 21.13; H, 5.32; N, 3.29. Found: C, 21.76; H, 5.25; N, 3.19%. For gas-sorption studies, a sample was evacuated at 250 °C for 20 h under dynamic vacuum at 10^{-5} Torr.

Compound **7**. Zinc (II) nitrate hexahydrate (Zn(NO$_3$)$_2$·6H$_2$O) (100 mg) and **3** (40 mg) were dissolved in DEF/DMF/ethanol/water (1:1:1:1 by volume) in a glass vial and then allowed to react at 80 °C for 24 h. Crystals of **7** were collected and washed with DMF and subsequently dried at 70 °C under vacuum to a afford white material (40% yield). Elemental analysis: *Anal*. Calc. for (C$_{26}$H$_{56}$B$_{40}$Zn$_2$O$_{10}$)·(2.25DMF): C, 31.31; H, 5.76; N, 2.51. Found: C, 32.62; H, 5.73; N, 2.45%. For gas-sorption studies, a sample was evacuated at 200 °C for 15 h under dynamic vacuum at 10^{-5} Torr.

3.3. Crystallographic studies

Single crystals were mounted on a BRUKER APEX2 V2.1-0 diffractometer equipped with a graphite-monochromated Mo Kα (λ = 0.71073 Å) radiation source in a cold nitrogen stream. All crystallographic data were corrected for Lorentz and polarization ef-

fects (SAINT), and face-index absorption corrections. The structures were solved by direct methods and refined by the full-matrix least-squares method on F2 with appropriate software implemented in the SHELXTL program package [21]. All the non-hydrogen atoms were refined anisotropically and added at their geometrically ideal positions (see Table 1 for refinement summary).

In the solid-state structure of **7**, most of the guest solvent molecules were severely disordered, which hindered their satisfactory refinement; therefore, the SQUEEZE routine (PLATON) was applied to remove the contributions of electron density from disordered solvent molecules [22]. The outputs from the SQUEEZE calculations are attached to the CIF file.

4. Conclusions

In summary, we have designed and synthesized new MOF materials using extended boron-rich ligands comprised of *p*-carborane building blocks. These materials are robust and can be activated thermally, resulting in highly porous structures. Indeed, to date these are the most porous carborane-based MOFs realized, and their properties point to potential use in gas separations.

Acknowledgements

Appendix A. Supplementary material

CCDC 773979 and 773980 contain the supplementary crystallographic data for **6** and **7**. These data can be obtained free of charge from The Cambridge Crystallographic Data Centre via http://www.ccdc.cam.ac.uk/data_request/cif.

Supplementary data associated with this article can be found, in the online version, at doi:10.1016/j.ica.2010.08.007.

Table 1
Crystal data and refinement summary for **6** and **7**.

Structure	6	7
Empirical formula	C$_{30}$H$_{87}$B$_{60}$N$_4$O$_{18}$Zn$_4$	C$_{26}$H$_{54}$B$_{40}$O$_{10}$Zn$_2$
Color	colorless	colorless
Crystal system	monoclinic	triclinic
Space group	$P_{2(1)/c}$	P_1
a (Å)	17.6825(4)	11.312(3)
b (Å)	22.3287(5)	16.930(4)
c (Å)	29.0317(6)	20.170(4)
α (°)	90.00	89.093(4)
β (°)	108.1000(10)	86.425(4)
γ (°)	90.00	88.896(4)
Z	4	2
D_x (Mg m^{-3})	1.038	0.939
Crystal size (mm)	0.134 × 0.123 × 0.015	0.209 × 0.097 × 0.091
Crystal shape	tabular	columnar
θ Range (°)	2.35–22.27	2.32–27.71
T (K)	153	153
Number of reflections measured	115,520	35,257
Number of unique reflections; R_{int}	13,623 (R_{int} = 0.1084)	17,825 (R_{int} = 0.1238)
Maximum and minimum transmission	0.9777 and 0.7691	0.8989 and 0.7695
Absorption correction	integration	integration
Refinement method	Full-matrix least squares on F^2	Full-matrix least squares on F^2
Final R indices [$I > 2\sigma(I)$]	R_1 = 0.0504, wR_2 = 0.1268	R_1 = 0.1016, wR_2 = 0.2465
R indices (all data)	R_1 = 0.0836, wR_2 = 0.1331	R_1 = 0.1384, wR_2 = 0.2641
$\Delta\rho$, maximum, minimum, (e Å^{-3})	0.799 and −0.533	5.688 and −1.178

References

[1] G. Ferey, Chem. Soc. Rev. 37 (2008) 191.
[2] L.J. Murray, M. Dincă, J.R. Long, Chem. Soc. Rev. 38 (2009) 1294.
[3] J.-R. Li, R.J. Kuppler, H.-C. Zhou, Chem. Soc. Rev. 38 (2009) 1477.
[4] J. Lee, O.K. Farha, J. Roberts, K.A. Scheidt, S.T. Nguyen, J.T. Hupp, Chem. Soc. Rev. 38 (2009) 1450.
[5] D.J. Tranchemontane, J.L. Mendoza-Cortés, M.J. O'Keeffe, O.M. Yaghi, Chem. Soc. Rev. 38 (2009) 1257.
[6] O.M. Yaghi, M. O'Keeffe, N.W. Ockwig, H.K. Chae, M. Eddaooudi, J. Kim, Nature 423 (2003) 705.
[7] M. Dincă, A. Dailly, Y. Liu, C.M. Brown, D.A. Neumann, J.R. Long, J. Am. Chem. Soc. 128 (2006) 16876.
[8] J. An, S. Geib, N.L. Rosi, J. Am. Chem. Soc. 132 (2010) 38.
[9] D. Britt, H. Furukawa, B. Wang, T.G. Glover, O.M. Yaghi, Proc. Natl. Acad. Sci. (USA) 106 (2009) 20637.
[10] A.P. Nelson, O.K. Farha, K.L. Mulfort, J.T. Hupp, J. Am. Chem. Soc. 131 (2009) 458.
[11] J. Plešek, Chem. Rev. 92 (1992) 269.
[12] O.K. Farha, A.M. Spokoyny, K.L. Mulfort, M.F. Hawthorne, C.A. Mirkin, J.T. Hupp, J. Am. Chem. Soc. 129 (2007) 12680.
[13] O.K. Farha, A.M. Spokoyny, K.L. Mulfort, S. Galli, J.T. Hupp, C.A. Mirkin, Small 5 (2009) 1727.
[14] Y.-S. Bae, O.K. Farha, A.M. Spokoyny, C.A. Mirkin, J.T. Hupp, R.Q. Snurr, Chem. Commun. (2008) 4135.
[15] A.M. Spokoyny, D. Kim, A. Sumrein, C.A. Mirkin, Chem. Soc. Rev. 38 (2009) 1218.
[16] Y.-S. Bae, A.M. Spokoyny, O.K. Farha, R.Q. Snurr, J.T. Hupp, C.A. Mirkin, Chem. Commun. 46 (2010) 3478.
[17] J. Müller, K. Baše, T.F. Magnera, J. Mich, J. Am. Chem. Soc. 114 (1992) 9721.

[18] U. Schoberl, T.F. Magnera, R.M. Harrison, F. Fleischer, J.L. Pflug, P.F.H. Schwab, X. Meng, D. Lipiak, B.C. Noll, V.S. Alluder, T. Rudalevige, S. Lee, J. Michl, J. Am. Chem. Soc. 119 (1997) 3907.
[19] X. Yang, W. Jiang, C. Knobler, M.F. Hawthorne, J. Am. Chem. Soc. 114 (1992) 9719.
[20] J.H. Cavka, S. Jakobsen, U. Olsbye, N. Guillou, C. Lamberti, S. Bordiga, K.P. Lillerud, J. Am. Chem. Soc. 130 (2008) 13850.
[21] G.M. Sheldrick, Acta Crystallogr., Sect. A64 (2008) 112.
[22] A.L. Spek, J. Appl. Crystallogr. 36 (2003) 7.